Elevated Convection Initiation on 24 June 2015 during PECAN: A Case Study

Scott Kehler[1] and John Hanesiak[1]

[1]Centre for Earth Observation Science, University of Manitoba, Winnipeg, Manitoba

INTRODUCTION

The development of convective storms after dark has long represented a challenge for forecasting as well as research. This is partly due to elevated storms forming above a stable planetary boundary layer (PBL) where few observations exist. In recognition of the need for more in-depth study of elevated convection, the Plains Elevated Convection at Night (PECAN; see Fig. 1) field project was conducted between 1 June and 15 July 2015 to improve our understanding of elevated convection. This poster shows some observations and model analysis of a case of elevated convection initiation on 24 June 2015 that was sampled during PECAN.

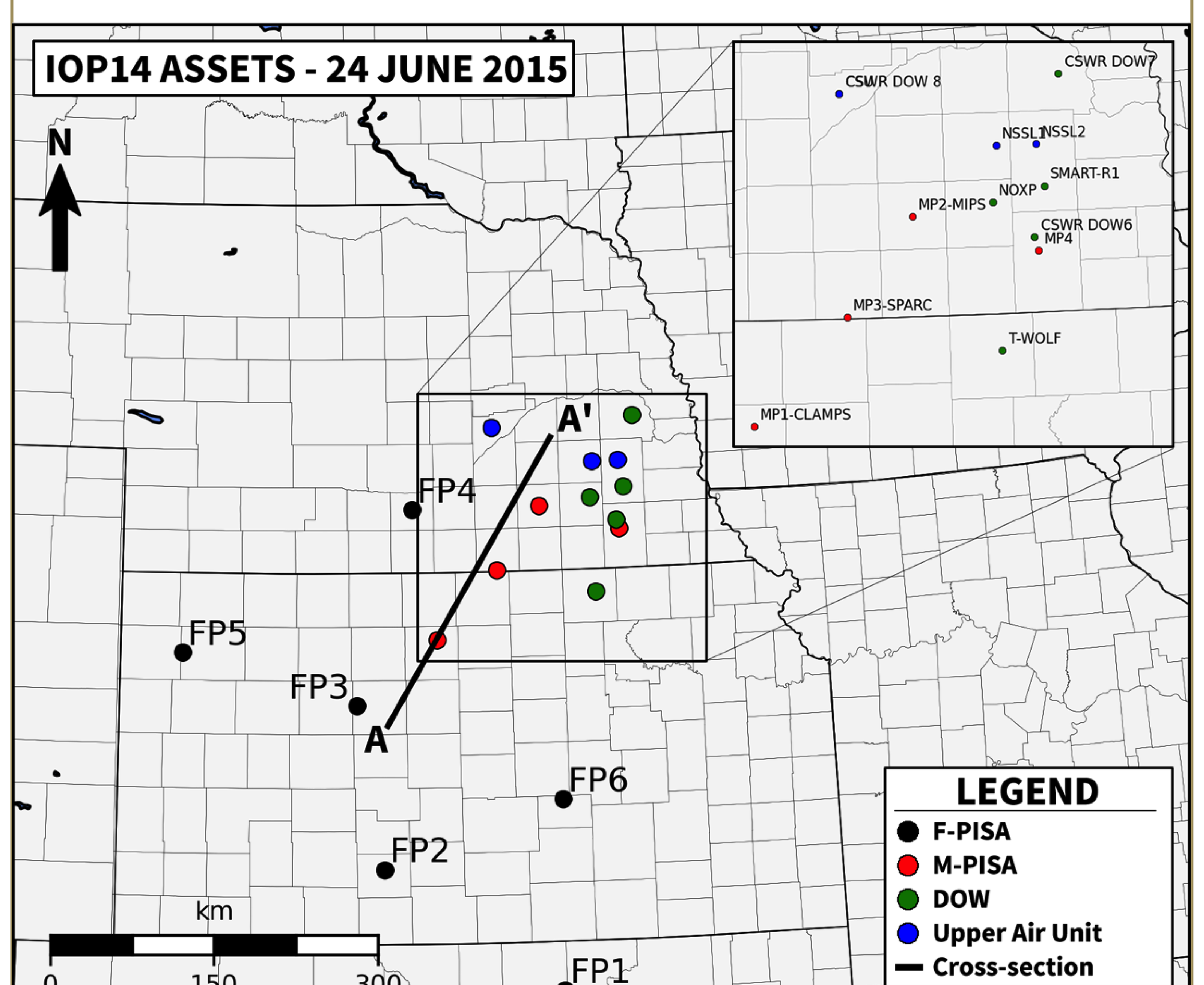

Fig. 1: The deployment of assets during IOP14 on 24 June 2015. The solid Black line from A to A' represents the vertical cross-section in Fig. 4.

DATA AND METHODS

The fourteenth IOP during PECAN was a combined convection initiation (CI)/low-level jet (LLJ) mission which sampled the environment near where elevated convection initiated poleward of a warm front in eastern Nebraska and western Iowa (see Fig. 2). Figure 1 shows the assets deployed for this case. Rawinsonde data was the primary PECAN dataset used in this research, supplemented by other operational datasets. This case was also simulated using the Weather Research and Forecasting (WRF) model to fill gaps in the observational data. The WRF was run at a horizontal grid spacing of 2 km with 50 vertical levels and a pressure top of 100 hPa.

DATA AND METHODS CONTINUED

The grid dimensions were 700 x 600, totaling 1400 km x 1200 km. No cumulus parameterization was used. Thompson microphysics, MYJ boundary-layer physics, and the Noah LSM were used for other parameterizations.

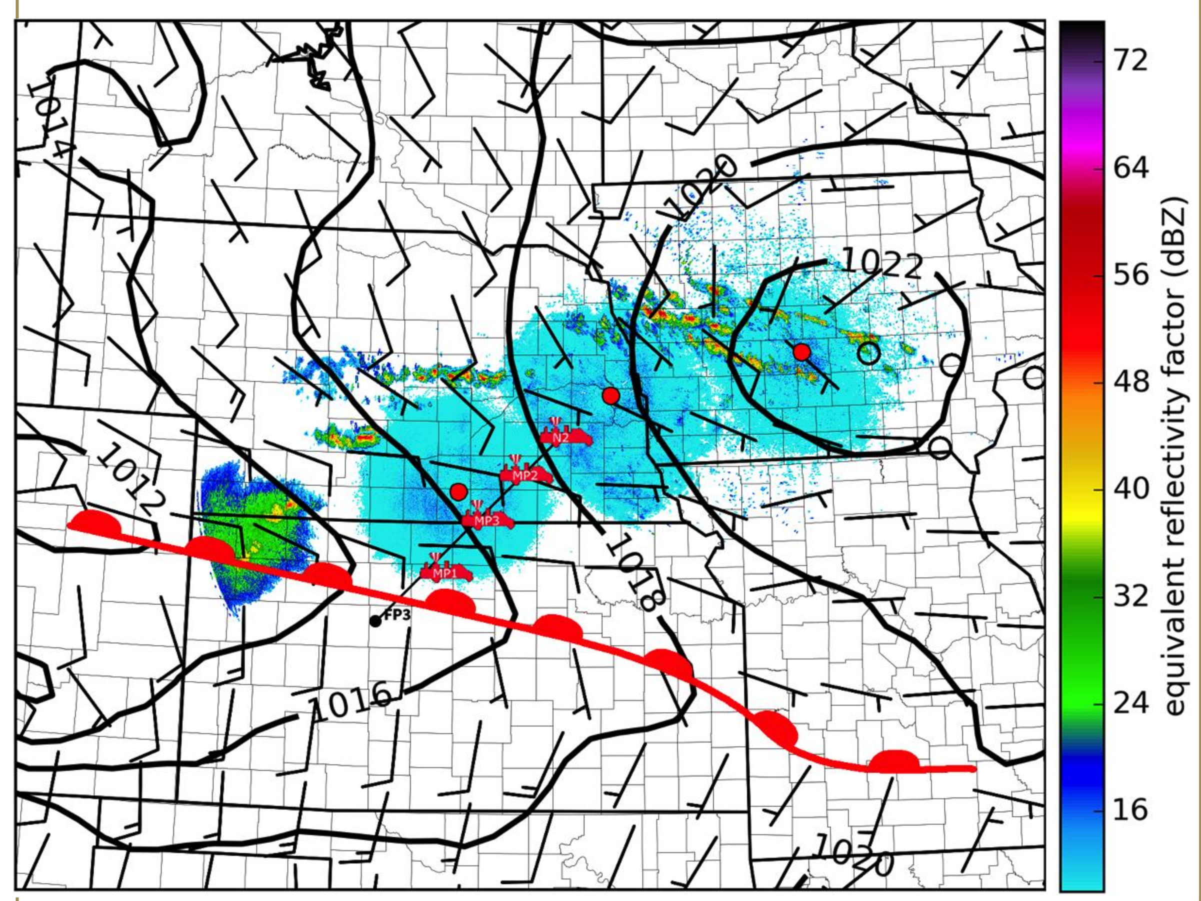

Fig. 2: The warm front on 24 June 2015, shown using the standard convention. Sea level pressure and surface winds were plotted from the NARR dataset (Mesinger 2006). The red icons represent the MPs used to construct the cross-sections in Fig. 4.

RESULTS

Convection initiated around 0500 UTC from pre-existing altocumulus castellanus clouds (ACC) over eastern NE/western IA, shown in Fig. 3. The slope of the warm front was calculated to provide information about the frontal structure and ascent. The average slope ranged from 1:180 at 0300 UTC to 1:320 at 0600 UTC, as depicted in Fig. 4. The frontal slope in the WRF simulation ranged from 1:130 at 0300 UTC to 1:220 at 0600 UTC. After sunset the vertical gradient in temperature and mixing ratio also appeared to increase in a thin layer.

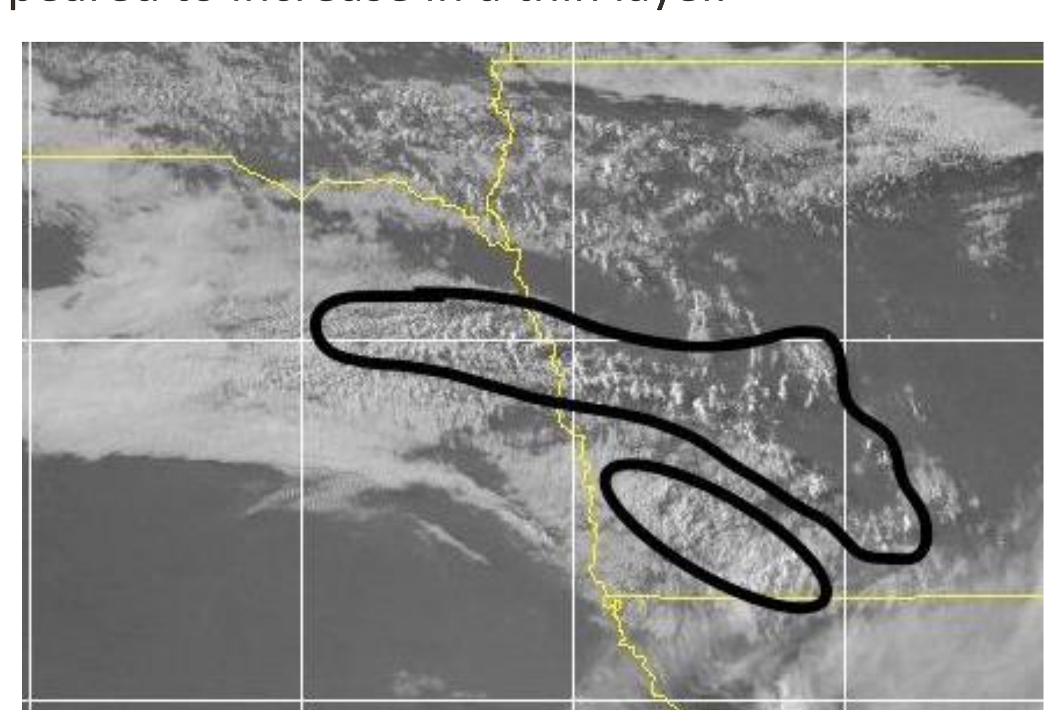

Fig. 3: Visible satellite image at 0000 UTC 24 June 2015 showing ACC.

RESULTS CONTINUED

A backward trajectory analysis was performed using the HYSPLIT model (Draxler and Hess 1998; Stein et al. 2015) with the NARR (Mesinger et al. 2006) dataset to determine the source region of the parcels that eventually produced the convection. The model was run over a 24-h period using isentropic and divergence-based vertical velocities. The trajectories primarily came from the OK/TX panhandles, with some originating in northern CO/southern WY. These trajectories are shown in Fig. 5.

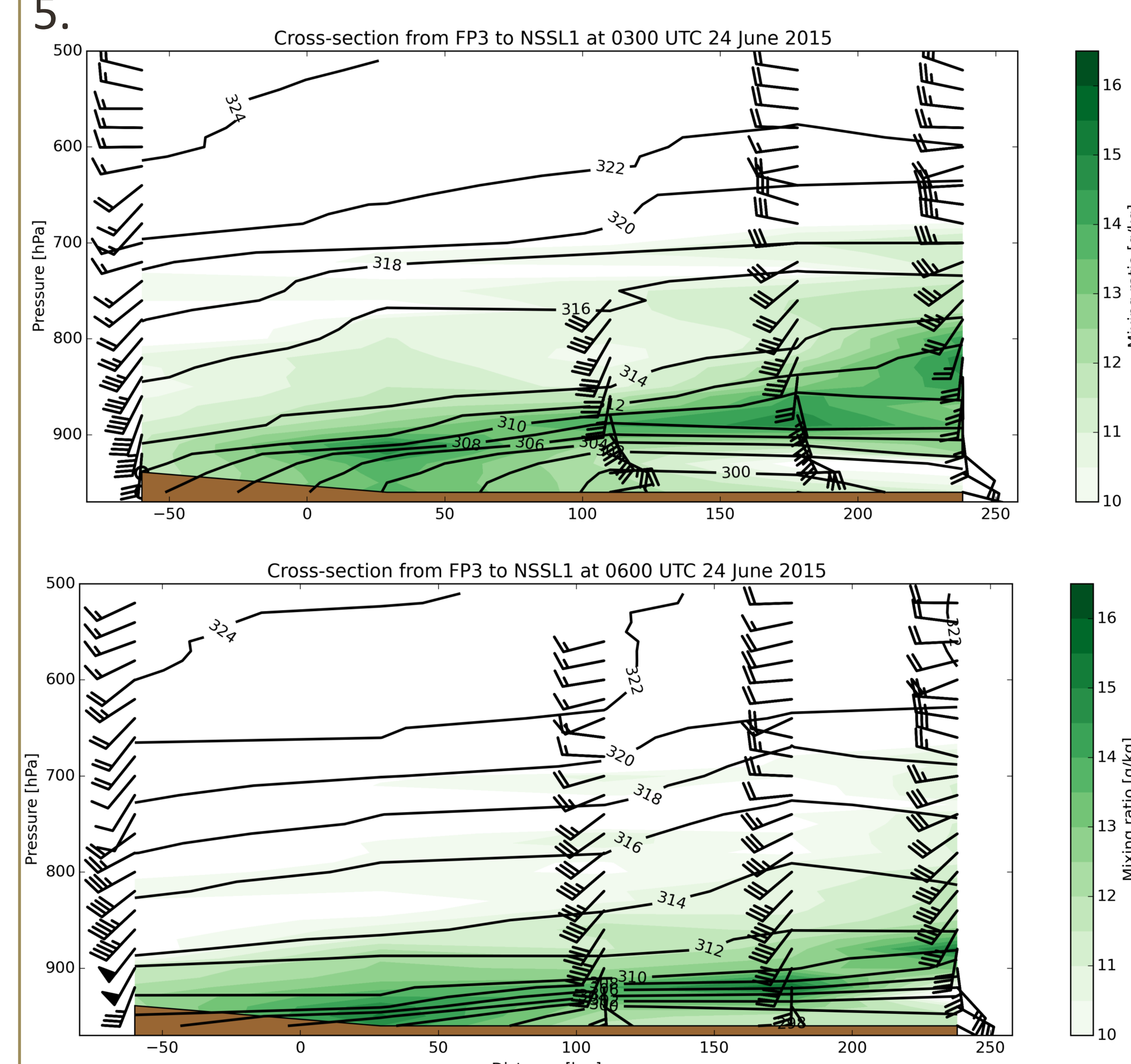

Fig. 4: (a) Cross-section along the line shown in Fig. 1 at 0300 UTC 24 June 2015. Solid contours are virtual potential temperature and shading is mixing ratio. (b) as in (a) but at 0600 UTC

Vertical velocities on the frontal surface were calculated to show regions of ascent relative to where the convection initiated. Kinematic vertical velocities were calculated using the technique of Davies-Jones (1993) and by vertically integrating the continuity equation. The surface and tropopause were assigned vertical velocities of zero to preserve mass continuity (Fankhauser 1969; OBrien 1970). The second technique to resolve vertical velocities used the vertical velocity equation in isentropic coordinates. Maximum kinematic vertical velocities were –12 $\mu b/s$ at 0300 UTC near 800 hPa, while maximum isentropic vertical velocities were -10 $\mu b/s$ at 0300 UTC. WRF kinematic vertical velocities are shown in Fig. 6.

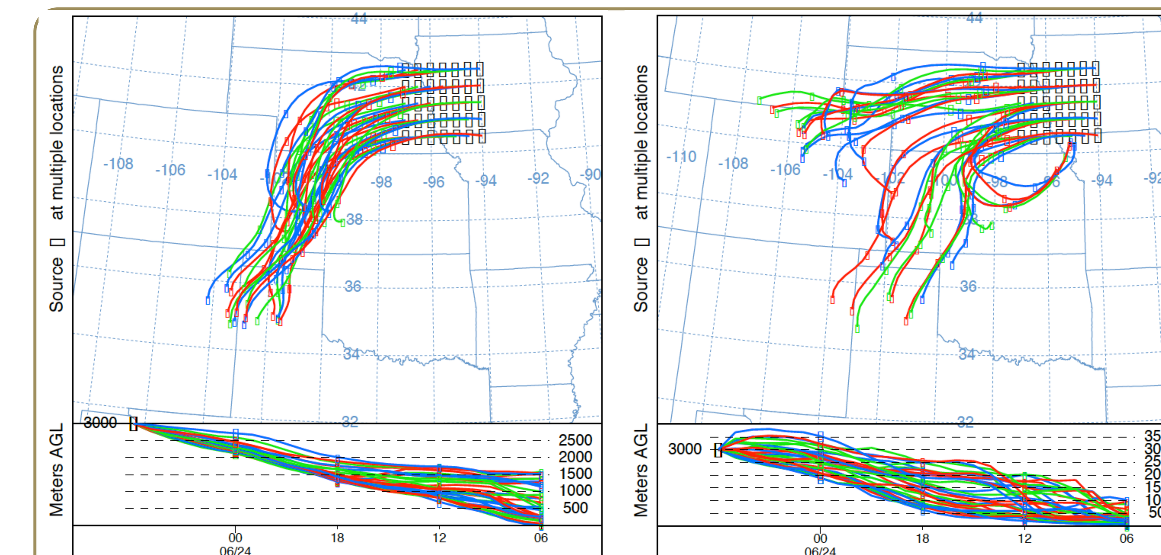

Fig. 5: (a) HYSPLIT backward trajectories at 0600 (red), 0300 (blue), and 0000 UTC (green) using isentropic vertical velocities. (b) as in (a) but using divergence to compute vertical velocities.

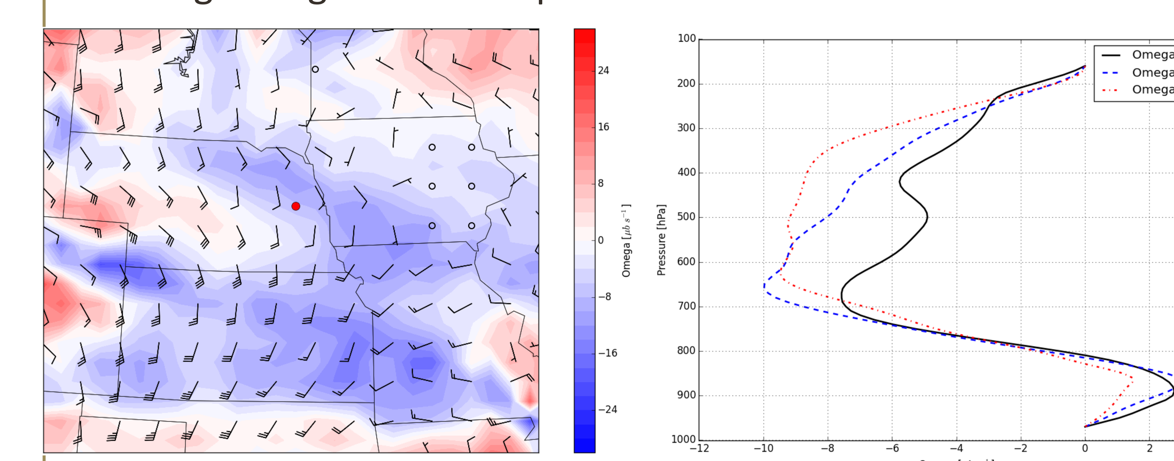

Fig. 6: (a) 700 hPa WRF kinematic vertical velocities (shaded) at 0400 UTC 24 June 2015. (b) Vertical profile of omega at the red dot shown in (a).

CONCLUSIONS

Both isentropic ascent and ascent from convergence along the low-level jet increased after sunset, helping to initiate elevated convection from a pre-existing deck of elevated convective clouds. Diurnal processes appeared to help confine a narrow, but rich stream of moisture to a thin layer along the frontal surface.

REFERENCES

Bellamy, J. C., 1949: Objective calculations of divergence, vertical velocity, and vorticity. *Bull. Amer. Meteor. Soc.*, 30, 45–49.

Davies-Jones, R., 1993: Useful formulas for computing divergence, vorticity, and their errors from three or more stations. *Mon. Wea. Rev.*, 121, 713–725.

Draxler, R. R. and G. D. Hess, 1998: An overview of the HYSPLIT 4 modelling system for trajectories, dispersion and deposition. *Aust. Met. Mag*, 47, 295–308.

Fankhauser, J. C., 1969: Convective processes resolved by a mesoscale rawinsonde network. *J. Appl. Meteor. Climatol.*, 8, 778–798.

Mesinger, F., G. DiMego, E. Kalnay, K. Mitchell, P. C. Shafran, W. Ebisuzaki, D. Jovíc, J. Woollen, E. Rogers, E. H. Berbery, M. B. Ek, Y. Fan, R. Grumbine, W. Higgins, H. Li, Y. Lin, G. Manikin, D. Parrish, and W. Shi, 2006: North American Regional Reanalysis. *Bull. Amer. Meteor. Soc.*, 87, 343–360.

OBrien, J. J., 1970: Alternative solutions to the classical vertical velocity problem. *J. Appl. Meteor. Climatol.*, 9, 197–203.

Stein, A. F., R. R. Draxler, G. D. Rolph, B. J. B. Stunder, M. D. Cohen, and F. Ngan, 2015: NOAA's HYSPLIT Atmospheric Transport and Dispersion Modeling System. *Bull. Amer. Meteor. Soc.*, 96, 2059–2077.

Trier, S. B. and D. B. Parsons, 1993: Evolution of environmental conditions preceding the development of a nocturnal mesoscale convective complex. *Mon. Wea. Rev.*, 121, 1078–1098.

ACKNOWLEDGEMENTS

Thanks goes to all those involved in PECAN for helping to collect the data used in this research – the names of those involved are too numerous to mention.